Supplementary Information for manuscript

Influence of NO and (NO)$_2$ Adsorption on the Properties of Fe-N4 Porphyrin-Like Graphene Sheet

Elham Ashori[1], Fariba Nazari[1,2*], Francesc Illas[3*]

[1]Department of Chemistry, Institute for Advanced Studies in Basic Sciences, Zanjan 45137-66731, Iran

[2]Center of Climate Change and Global Warming, Institute for Advanced Studies in Basic Sciences, Zanjan 45137-66731, Iran

[3]Departament de Ciència de Materials i Química Física & Institut de Química Teòrica i Computacional (IQTCUB), Universitat de Barcelona, C/Martí i Franquès 1, 08028 Barcelona, Spain

Definition of the various defects studied in the present work

On the graphene supercell considered in the present work, defect formation can be represented through Eq. (S1)

$$C_{60} + \frac{x}{2}N_2 + TM \rightarrow C_{60-x-y}N_x TM + (x+y)C \tag{S1},$$

whereas the formation energy is computed as in Eq. (S2)

$$\Delta E = E_{C_{60-x-y}N_x TM} + (x+y)\mu_C - \left[E_{C_{60}} + x\mu_N + E_{TM(g)} \right] \tag{S2},$$

and the binding energy of a transition metal atom to the P-N4 structure is as in Eq. (S3)

$$BE = E_{C_{60-x-y}N_x TM} - \left[E_{C_{60-x-y}N_x} + E_{TM(g)} \right] \tag{S3}.$$

The meaning of the various quantities in Eqs. S1-S3 is as for Eqs. 1-3 in the main text. Results concerning ΔE and BE for the various defects studied in the present work are summarized in Tables S1 to S5 where comparison to available previous results is included for comparison

Table S1

Defect formation energies (ΔE in eV) and magnetic moments (m in μ_B) of in-plane defects in Graphene. Notation is as in the main text. Values in parentheses correspond to the reference [1].

Defect	DV	Py-N	P-N3	P-N4	G-Fe-N4
ΔE	8.06	5.82	3.64	4.05	-2.98
	(8.51)	(5.88)	(3.53)	(3.99)	(-3.09)
m	0.00	1.00	0.50	0.00	2.00
	(0.00)	(1.00)	(0.46)	(0.00)	(2.00)

Table S2

Binding energy (BE in eV) and bond lengths (d in Å) for the optimized equilibrium geometry of G-Fe-N4. C1 and C2 correspond to carbon atom of rings five and six for Fe-N4 defect, respectively.

	BE	d_{Fe-N}	d_{N-C1}	d_{N-C2}
G-Fe-N4	-7.73	1.89	1.38	1.39
	-7.07 [1]	1.900 [2]	1.380 [2]	1.392 [2]

Table S3

Calculated and available experimental structure parameters of acyclic cis-ONNO ($^1A_1$, $^3A_1$) and trans-ONNO ($^1A_1$, $^3A_1$) and cyclic rectangular ONON ($^1A_1$, $^3A_1$). Distances (d) are in Å and angles in degrees.

	d_{N-N}	d_{N-O}	$\angle$(ONN)	$\angle$(ONO)	d_{N-O}^a d_{N-O}^b
cis-ONNO ($^1A_1$)	2.03	1.17	100.4		
	2.013[c] [3]	1.176[c] [3]	98.5[c] [3]	–	–
	2.263[d] [4]	1.1515[d] [4]	97.17[d] [4]		
cis-ONNO ($^3A_1$)	1.99	1.17	111.0		
	1.917[c] [3]	1.180[c] [3]	108.8[c] [3]	–	–
	2.237[d][5]	1.161[d] [5]	99.6[d] [5]		
trans-ONNO ($^1A_1$)	1.21	1.22	145.1		
	1.864[c] [3]	1.182[c] [3]	106.6[c] [3]	–	–
trans-ONNO ($^3A_1$)	1.96	1.17	114.0		
	1.830[c] [3]	1.183[c] [3]	111.6[c] [3]	–	–
ONON ($^1A_1$)	–	–	–	85.4	1.16[a]
				90.0	2.28[b]
ONON($^3A_1$)	–	–	–	85.9	1.16[a]
				86.3	2.44, 2.45[b]

[a] Short NO bond length in the cyclic parallelogram structure.

[b] Long NO bond length in the cyclic parallelogram structure

[c] Predicted by DFT based calculations with the PBE functional

[d] Experimental values

Table S4

The adsorption energies (E_{ads}), dimer formation energies (E_{dim}), reconstruction energies (E_{rec}) and binding energies (E_{bin}) of adsorption complex ($ACII_1$-$ACII_5$). Values in parenthesis correspond to results without dispersion terms. All values are in eV.

	$ACII_1$	$ACII_2$	$ACII_3$	$ACII_4$	$ACII_5$
E_{ads}	-3.20	-2.91	-2.31	-1.84	-4.89
	(-2.86)	(-2.61)	(-2.10)	(-1.58)	(-4.61)
E_{dim}	-2.12	-0.51	-0.17	-0.45	–
	(-1.98)	(-0.34)	(-0.11)	(-0.33)	
E_{rec}	0.89	0.74	0.44	0.23	1.38
	(0.90)	(0.76)	(0.45)	(0.25)	(1.45)

Table S5

Bond lengths (d in Å) and magnetic moments (m in μ_B) of NO dimer adsorbed on the G-Fe-N4 in five stable configurations ($ACII_1$- $ACII_5$). Δz is the out-of-plane dislocation of the metal atom in Å. Values in parenthesis correspond to results without dispersion terms. C1 stands for the carbon atom of ring five.

	d_{Fe-N}	d_{N-C1}	d_{N-C2}	d_{N-N}	d_{N1-O1}, d_{N2-O2} d_{N1-O2}, d_{N2-O1}	d_{Fe-X} X=O,N	m	Δz
$ACII_1$	1.92,1.94,1.95, 1.96 (1.92,1.94,1.95, 1.96)	1.36,1.37 (1.36,1.37)	1.38,1.39 (1.38,1.39)	1.28 (1.28)	1.25,1.38 (1.25,1.38)	d_{Fe-O} 1.92 (1.92)	0.0 (0.0)	0.52 (0.53)
$ACII_2$	1.93,1.94,1.95 (1.94,1.95)	1.37 (1.37)	1.38,1.39 (1.38,1.39)	1.27 (1.27)	1.25, 1.25 (1.25, 1.25)	d_{Fe-N} 1.91 (1.92)	1.00 (1.00)	0.48 (0.49)
$ACII_3$	1.94, 1.92 (1.94, 1.92)	1.37 (1.37)	1.38 (1.38)	–	1.19, 1.17 2.86, 2.76 (1.19,1.17 2.94,2.91)	d_{Fe-N} 1.68 (1.68)	1.50 (1.50)	0.39 (0.40)
$ACII_4$	1.90,1.91 (1.90,1.91,1.92)	1.37 (1.37)	1.39 (1.39)	1.94 (1.94)	1.20, 1.16 (1.20,1.16)	d_{Fe-N} 1.75 (1.75)	0.0 (0.0)	0.31 (0.32)
$ACII_5$	1.96, 2.02 (1.96, 1.97, 2.02)	1.37 (1.37)	1.38 (1.38)	1.25 (1.25)	1.36, 1.36 (1.36,1.36)	d_{Fe-O} 1.90 (1.90)	1.00 (1.00)	0.66 (0.66)

TableS6

Bond lengths (Å) and bond angle (º) for N_2O, N_2 and O_2. Values in parentheses correspond to experiment.

Molecules	d_{N-N}	d_{N-O}	d_{O-O}	$\angle ONN$
N_2O	1.14, (1.129) [6]	1.20, (1.188) [6]	-	180.0, (180.0) [6]
N_2	1.11, (1.098) [7]	-	-	-
O_2	-	-	1.23, (1.208) [7]	-

Fig. S1 Configurations (a) pristine graphene, (b) double vacancy (DV), (c) pyrrolic N (Py-N), (d) pyridinic N3 (P-N3), (e) pyridinic N4 (P-N4) and (f) G-Fe-N4.
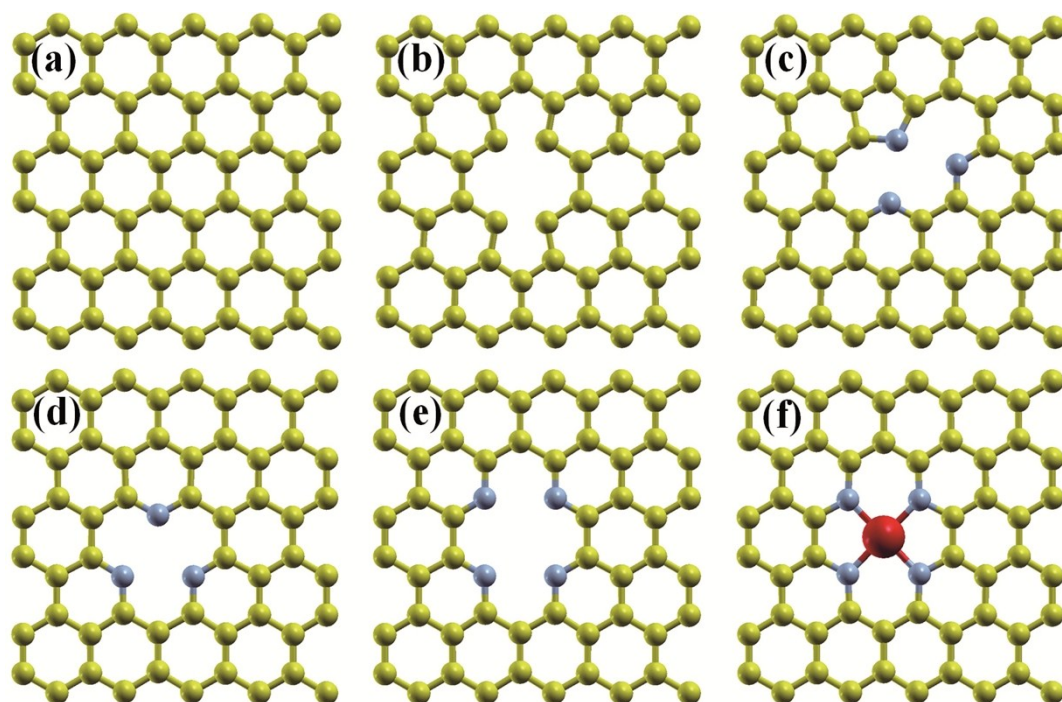
Fig. S2 Spin-resolved (a) band structures, (b) DOS, (c) LDOS of four N atom, ten carbon atoms and Fe atom, (d) PDOS of Fe atom, and (e) PDOS of N atom and (f) spin density plot for G-Fe-N4 surface. (The arrows denote majority spin (↑) and minority spin (↓) states.)
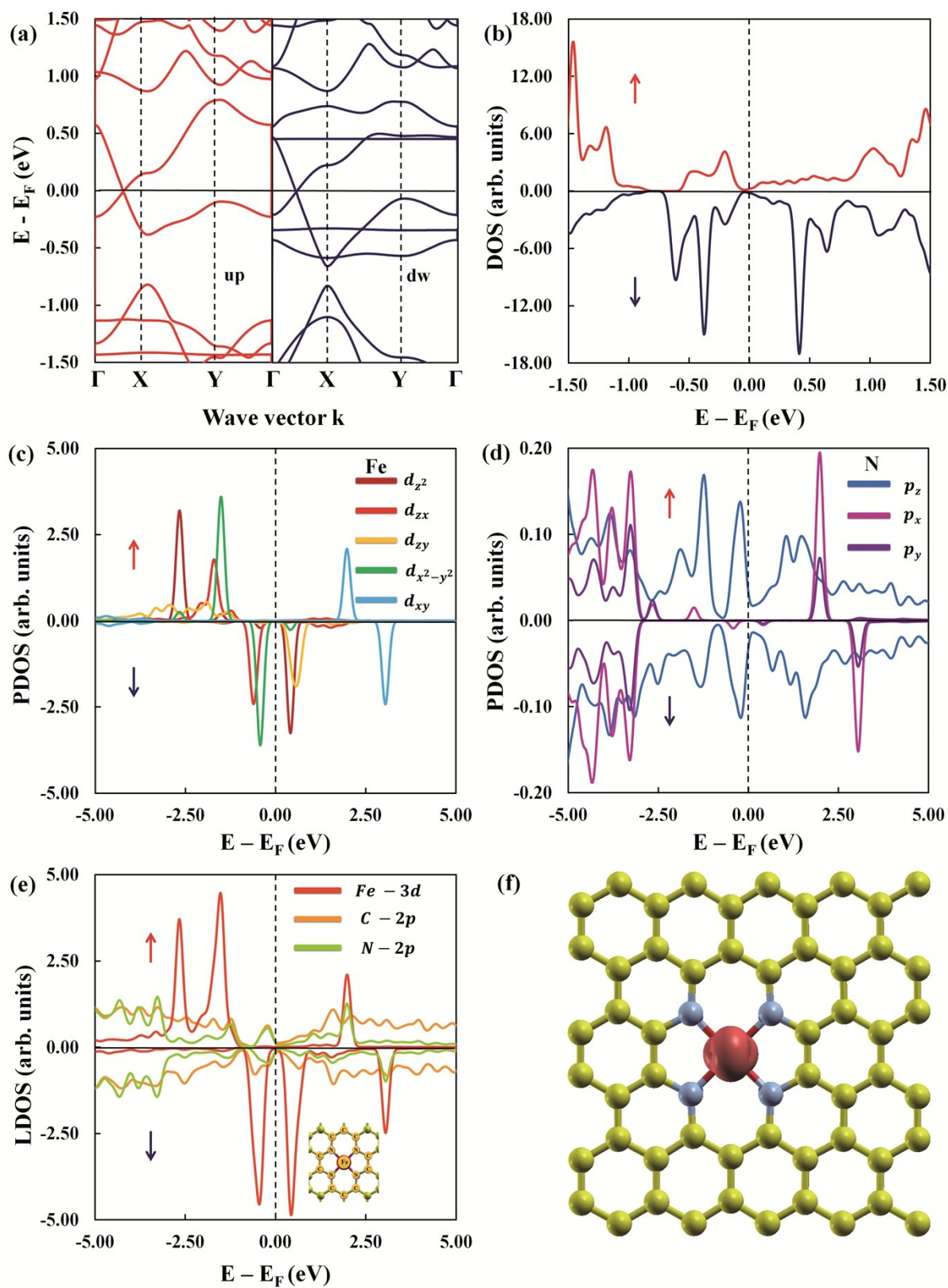
Fig. S3 Spin-resolved (a) DOS, (b) spin density plot (c) PDOS of N atom and (d) PDOS of O atom for NO molecule. (The arrows denote majority spin (↑) and minority spin (↓) states.)
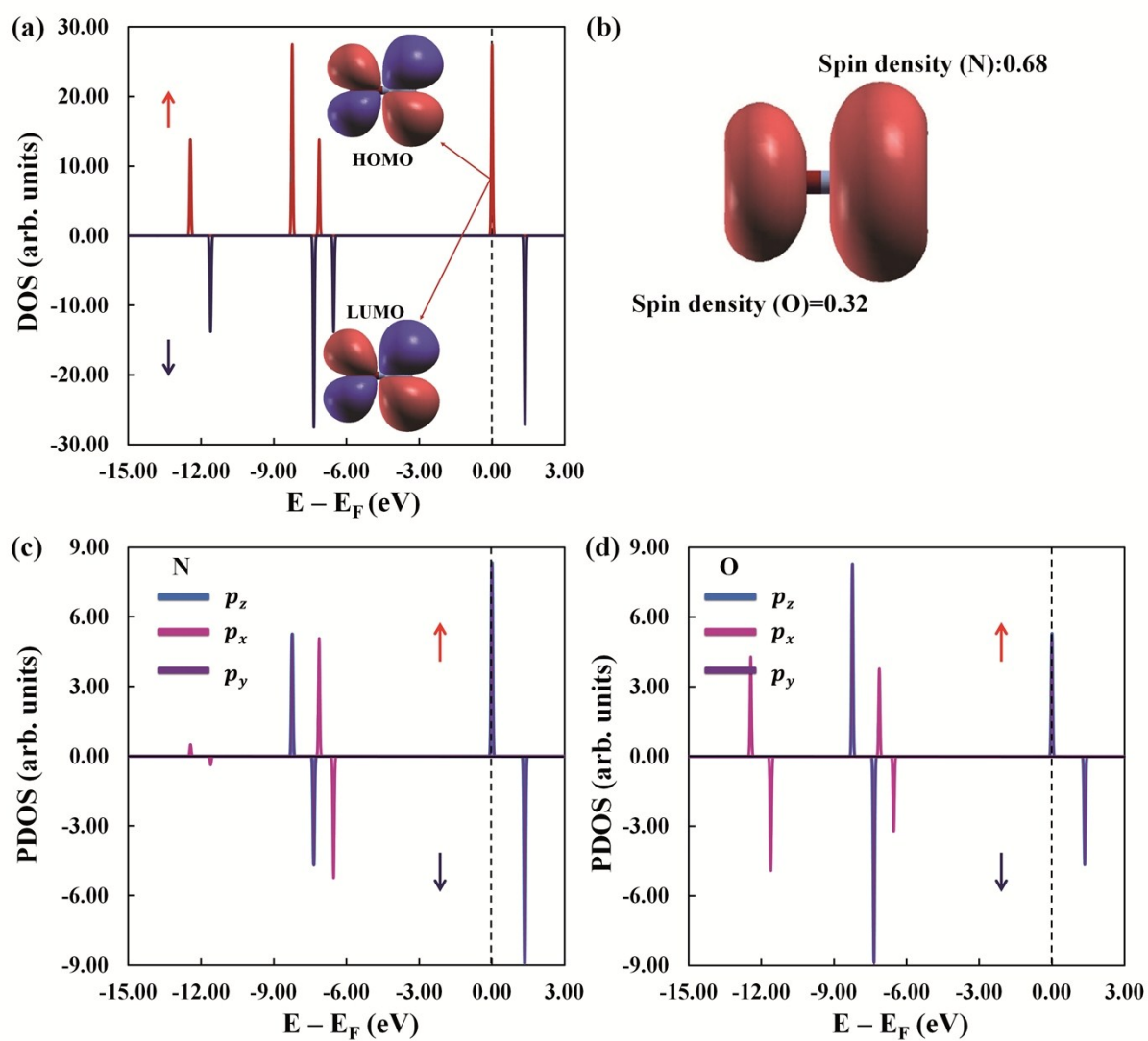
Fig. S4 Optimized geometries of possible ground states for the NO dimer (a) acyclic cis-ONNO ($^1A_1$), (b) acyclic cis-ONNO ($^3A_1$), (c) acyclic trans-ONNO ($^1A_1$), (d) acyclic trans-ONNO ($^3A_1$), (e) cyclic NONO ($^1A_1$; rectangle), and (f) cyclic NONO ($^3A_1$; rectangle).

Acyclic cis-ONNO ($^1A_1$) Acyclic trans-ONNO ($^1A_1$) Cyclic NONO ($^1A_1$; rectangle)

Acyclic cis-ONNO ($^3A_1$) Acyclic trans-ONNO ($^3A_1$) Cyclic NONO ($^1A_1$; rectangle)
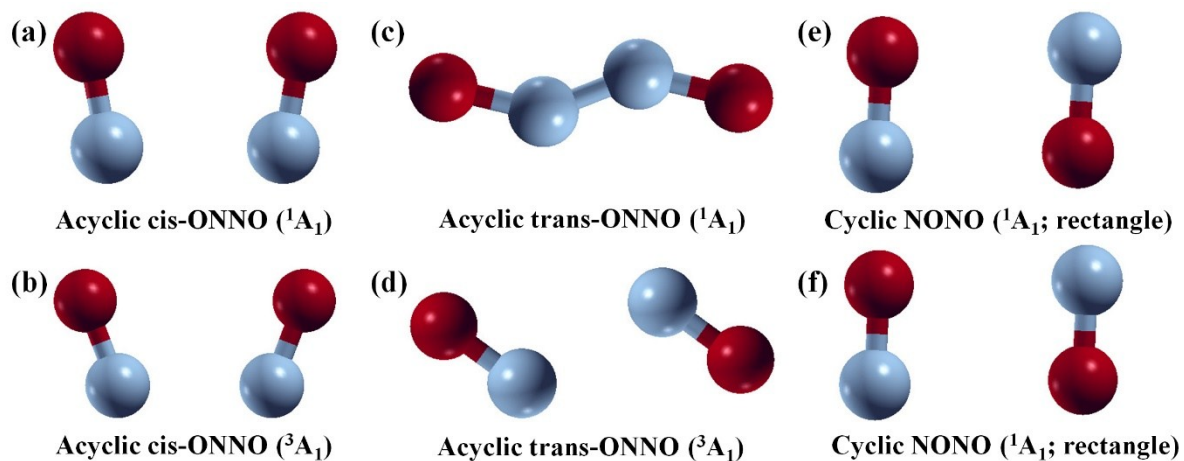
Fig. S5 Binding energy of optimized geometries of possible ground states for the isolated (NO)$_2$ dimer.
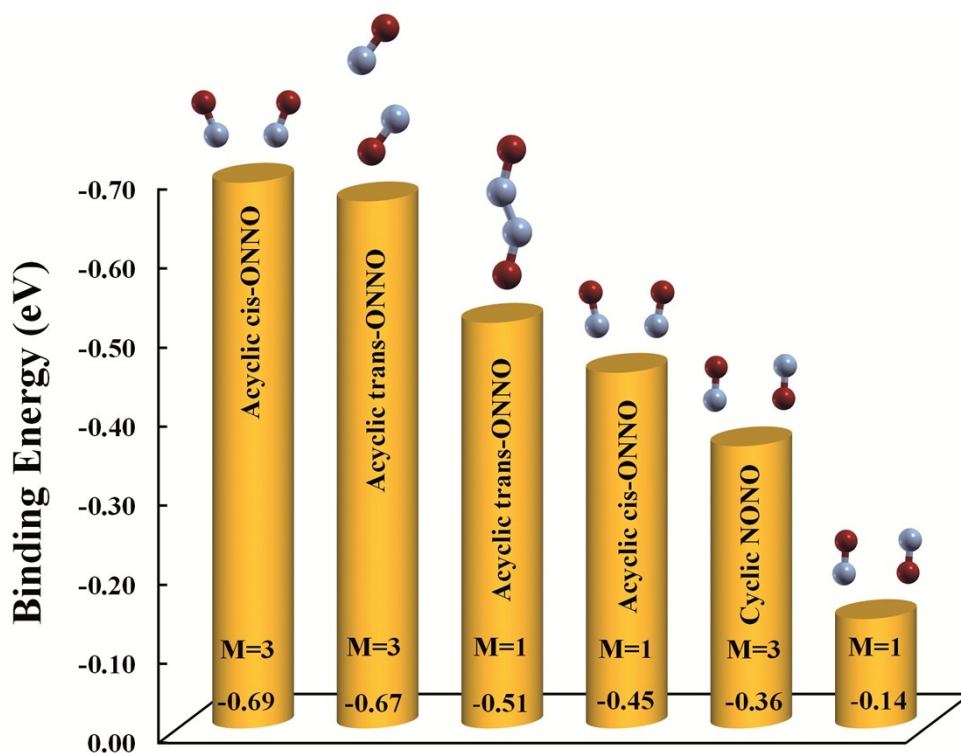
Fig. S6 Spin-resolved (a) DOS, (b) spin density (c) PDOS of O atom and (d) PDOS of N atom for acyclic cis-ONNO ($^3A_1$). (The arrows denote majority spin (↑) and minority spin (↓) states.).
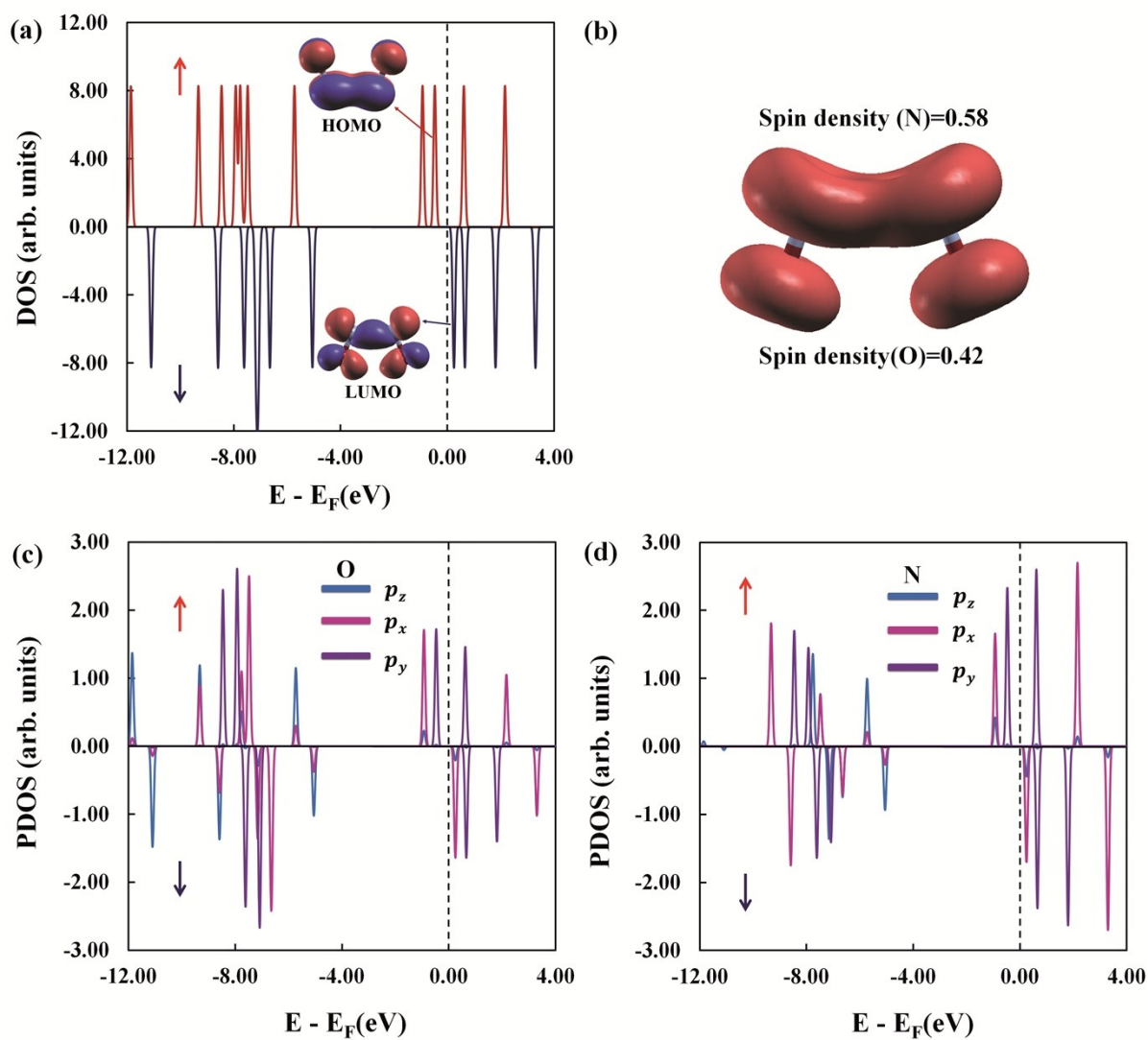
Fig. S7 Adsorption energies of NO molecule on pristine graphene (Gr), pyridinic N4 (P-N4), and G-Fe-N4 surfaces.
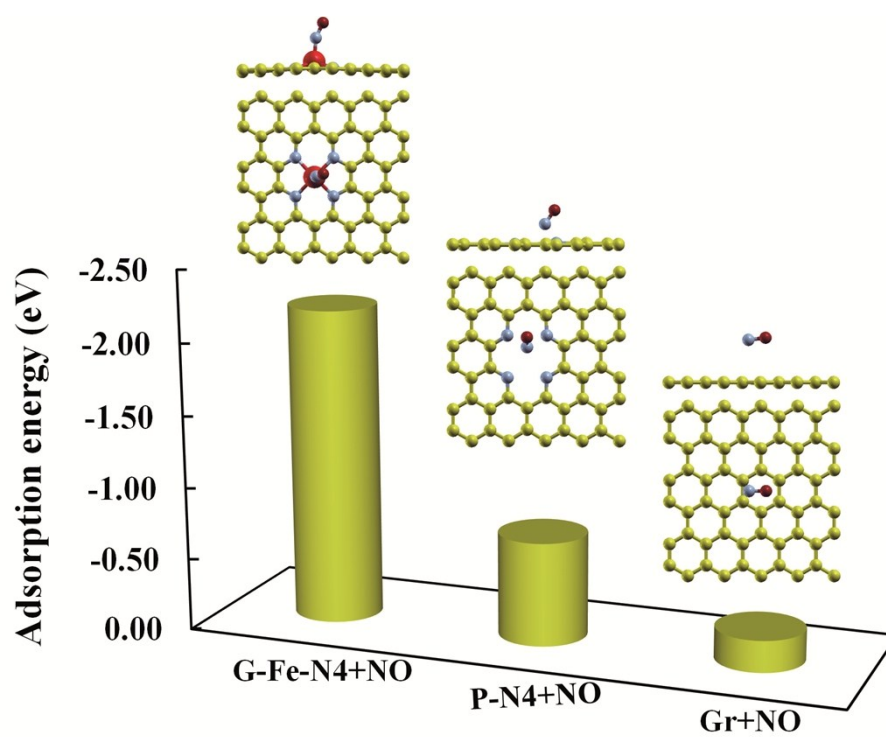
Fig. S8 The 2D plot of the electron localization functions (ELFs) of ACI_1.
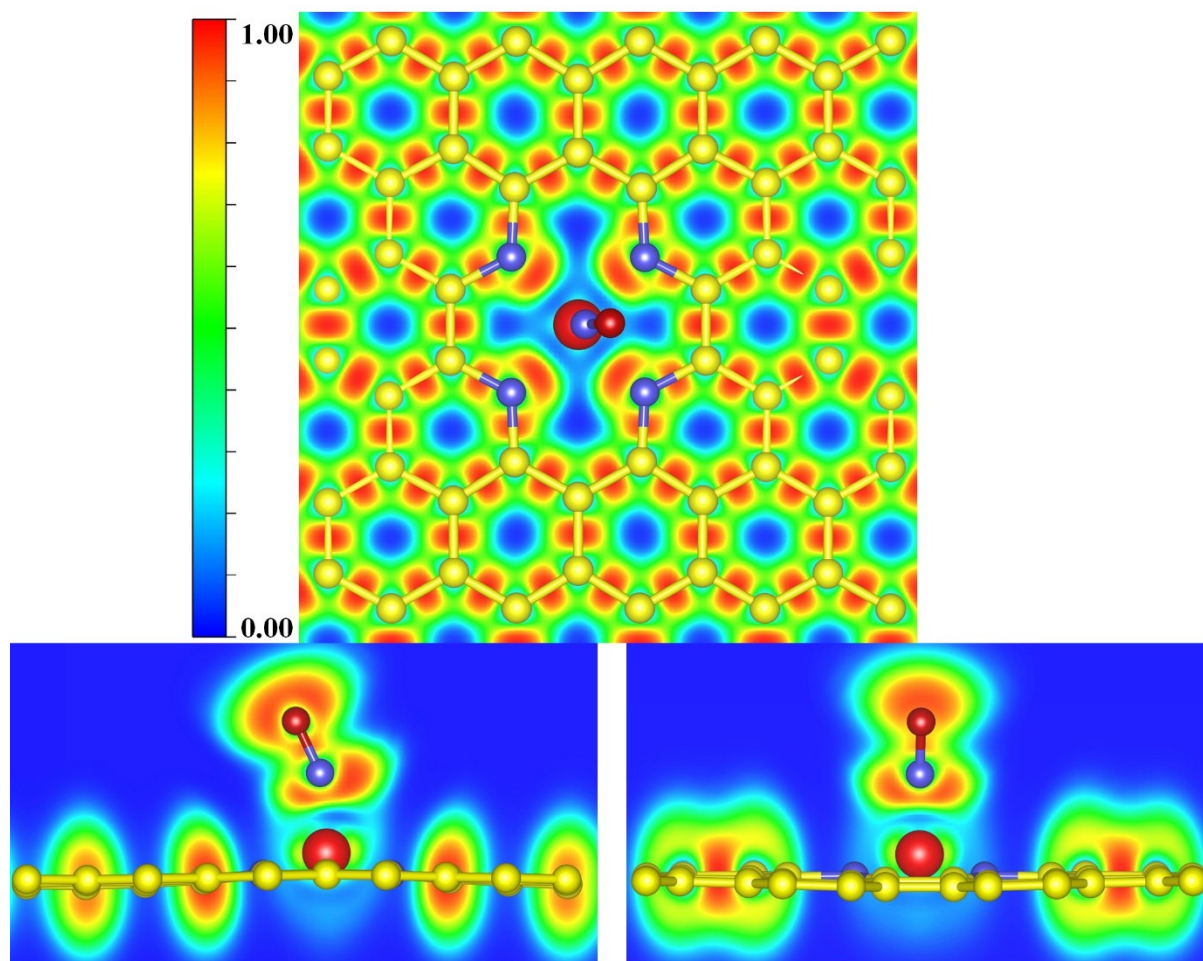
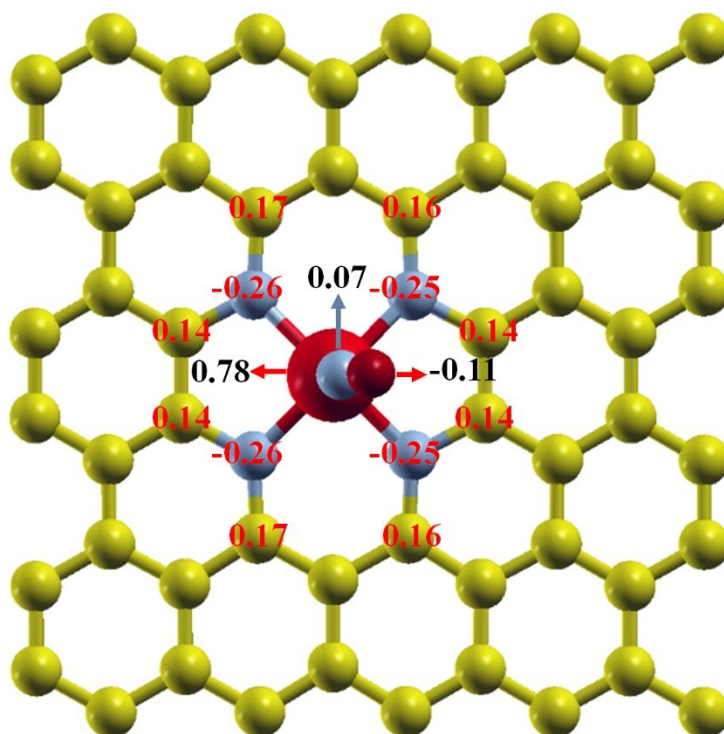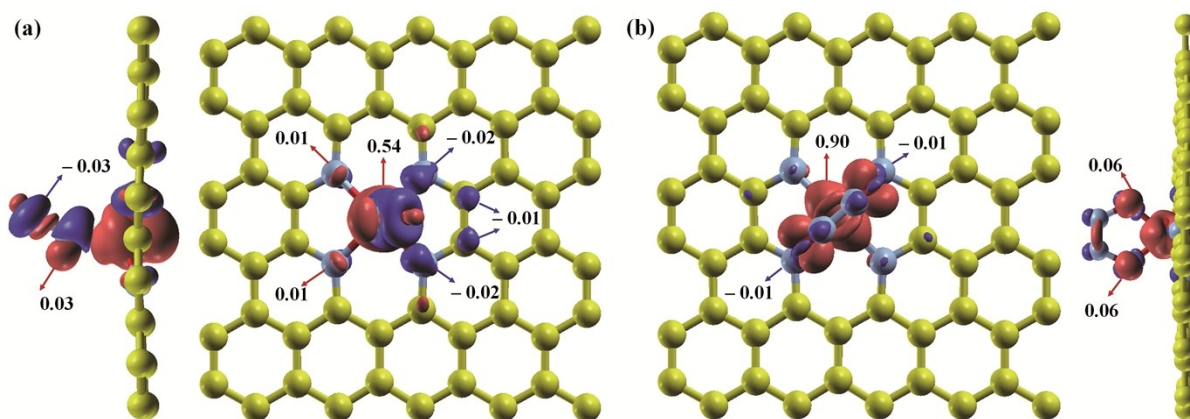**Fig. S9** Calculated net charges from Löwdin population analysis of ACI_1 (in e).

Fig. S10 (a) Spin density plot including spin density in some atoms for (a) ACI$_1$ and (b) ACII$_5$.
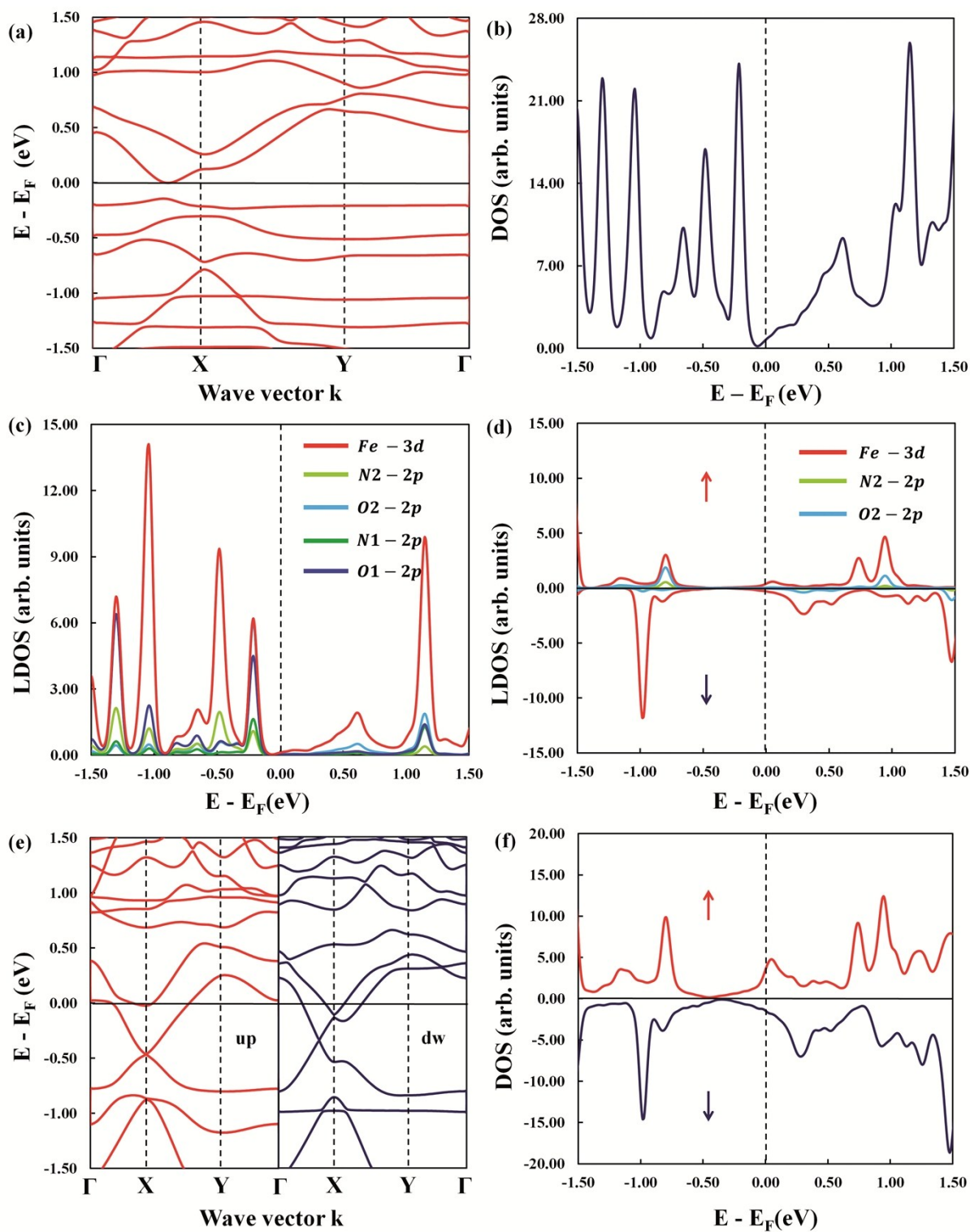

Fig. S11 Spin-resolved PDOS for (a) Fe atom (d_{z^2}, d_{zx}, d_{zy} and d_{xy} orbitals), (b) Fe atom ($d_{x^2-y^2}$ orbital), (c) N atom of NO molecule (p_z, p_x and p_y orbitals), and (d) O atom of NO molecule (p_z, p_x and p_y orbitals) of ACI$_1$. The arrows denote majority spin (↑) and minority spin (↓) channels.
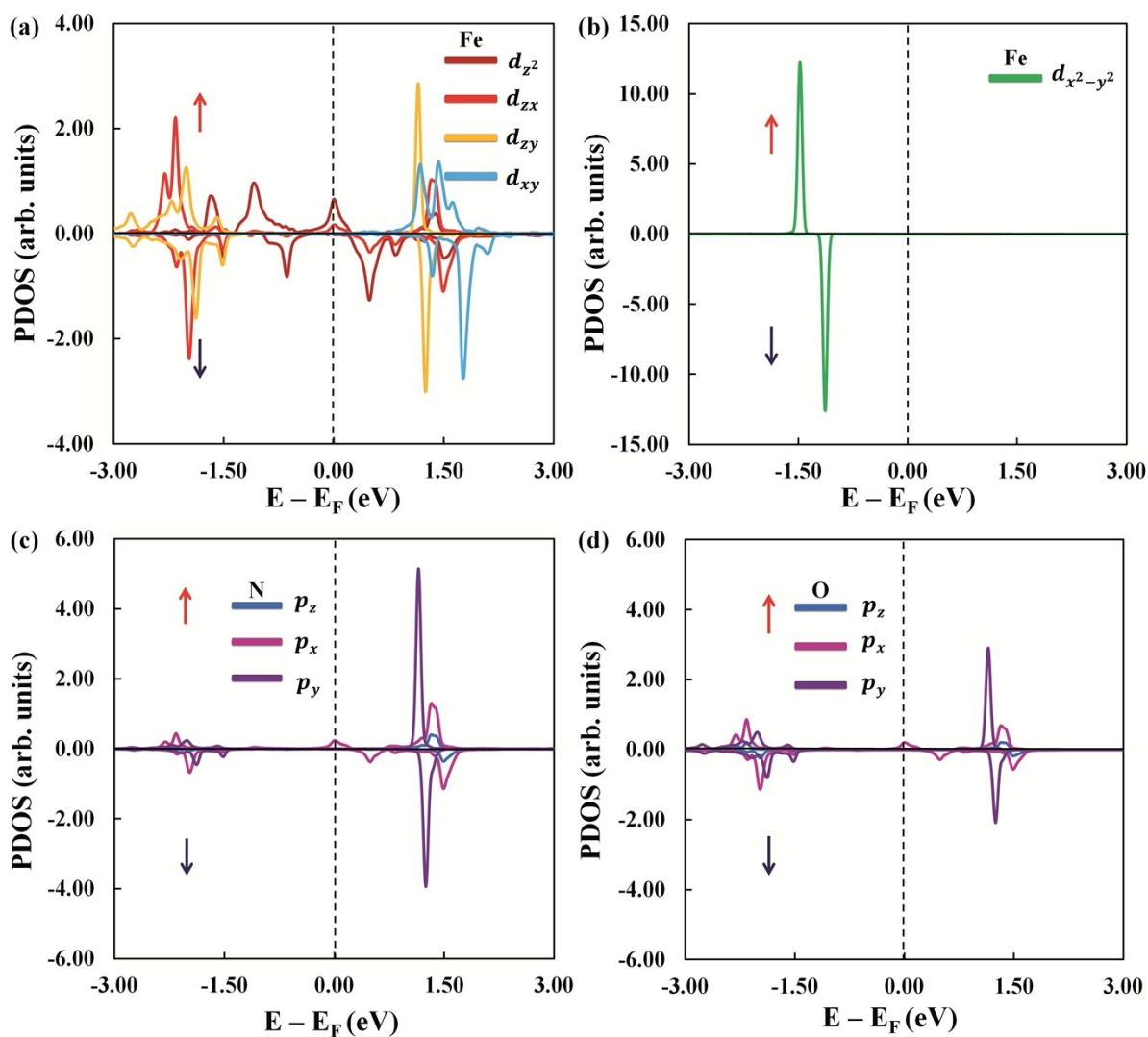
Fig. S12 Six different initial orientations of acyclic cis-ONNO ($^3A_1$) on the pristine G-Fe-N4 surface.
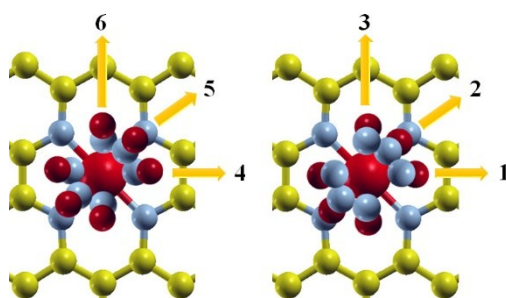
Fig. S13 Adsorption energy (E_{ads}), dimer formation energy (E_{dim}), and reconstruction energy (E_{rec}) of adsorption complexes (ACII$_1$-ACII$_5$) with and without dispersion correction. (Adsorption energy and dimer formation energy are multiply by -1 for better representation).
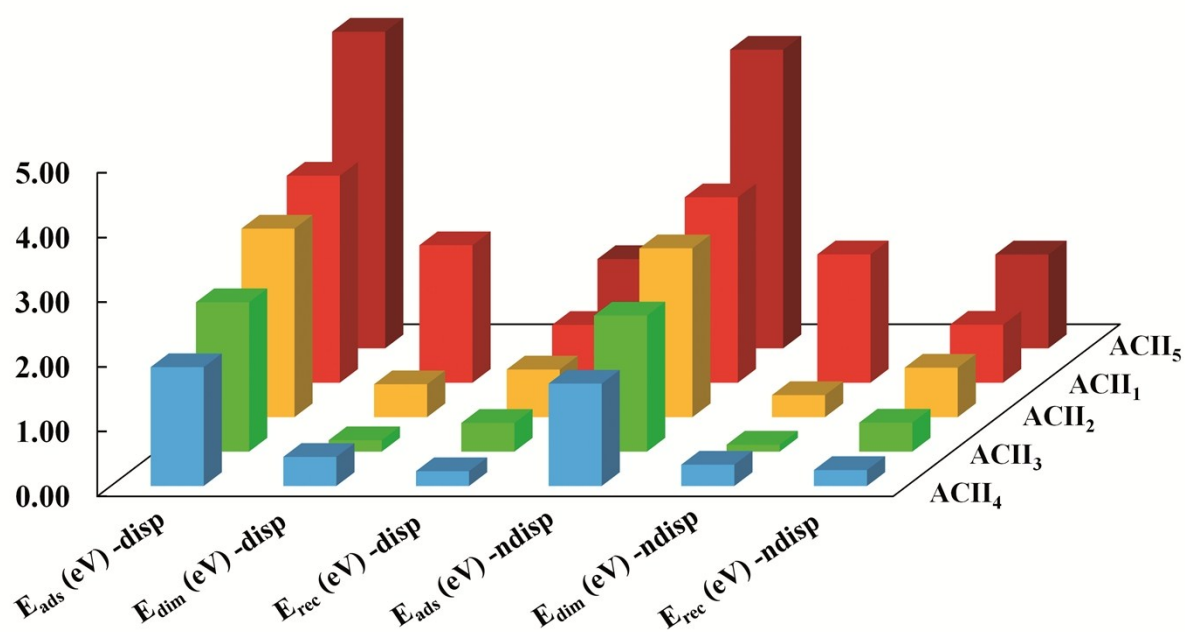
Fig. S14 Spin-unpolarized (a) electronic band structure, (b) DOS, and (c) LDOS (Fe, N2, O2, N1 and O1 atoms) for $ACII_1$ and spin-polarized (d) LDOS (Fe, N2 and O2 atoms), (e) electronic band structure, and (f) DOS for $ACII_5$. (The arrows denote majority spin ($\uparrow$) and minority spin ($\downarrow$) channels.)

Fig. S15 Spin-resolved PDOS for (a) Fe atom (d_{z^2}, d_{zx}, d_{zy} and d_{xy} orbitals), (b) Fe atom ($d_{x^2-y^2}$ orbital), (c) N atom of NO molecule (p_z, p_x and p_y orbitals), and (d) O atom of NO molecule (p_z, p_x and p_y orbitals) for ACII$_5$. The up and down arrows denote majority spin ($\uparrow$) and minority spin ($\downarrow$) channels.
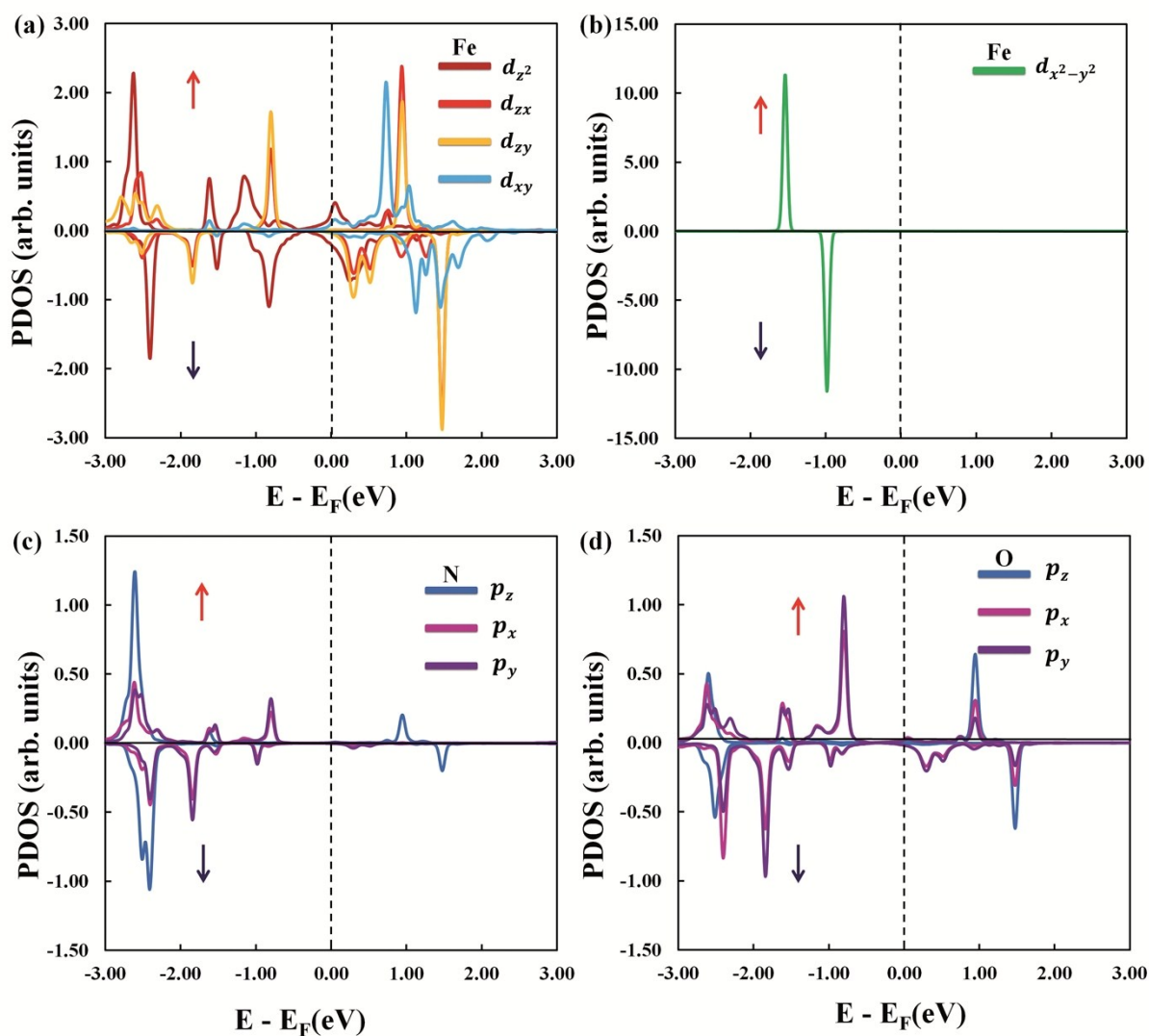
Fig. S16 Energy profile for direct decomposition NO on the G-Fe-N4 surface. All energies are reported in eV relative to the initial state (IS_a) and distances are in Å.
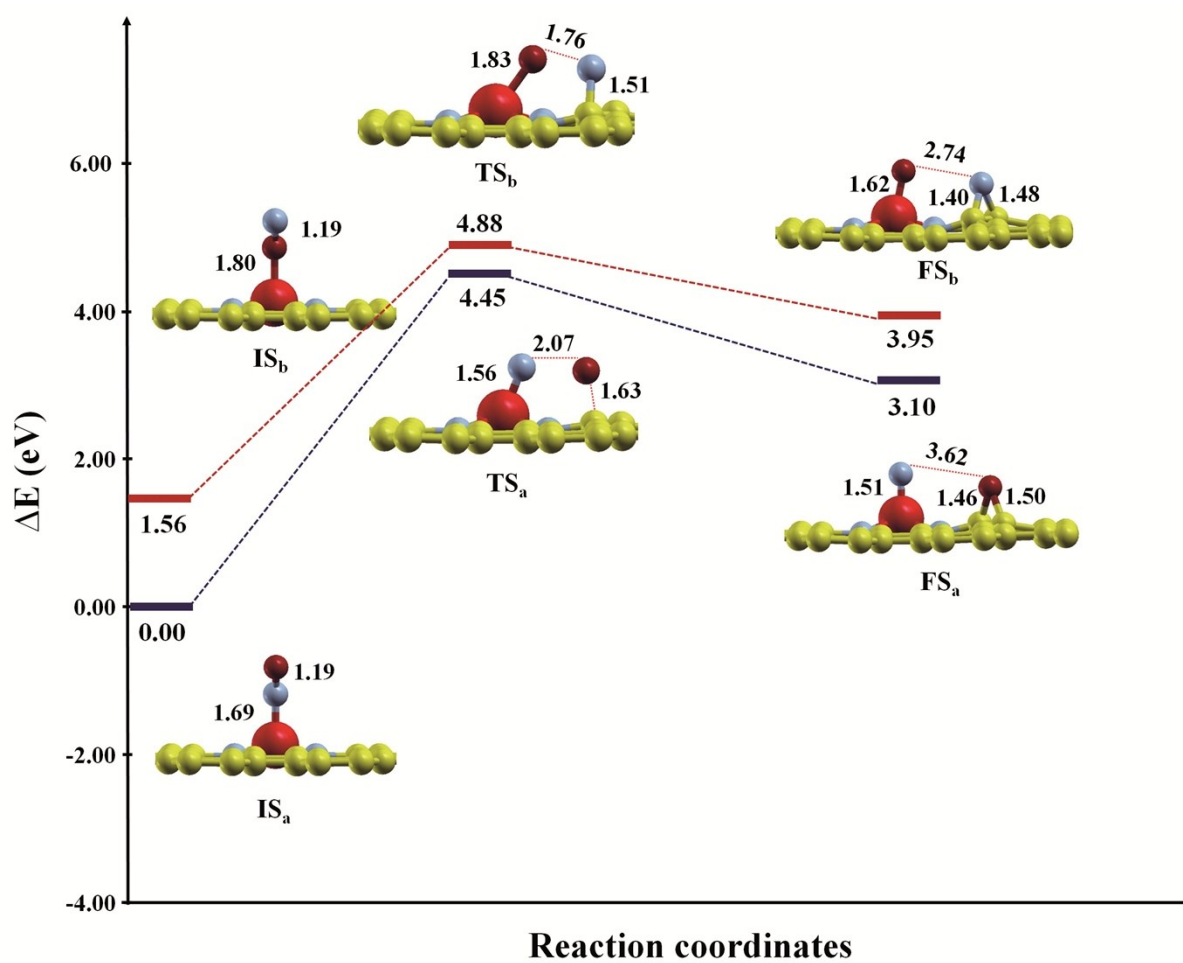
Fig. S17 Energy profile for interconversion of ACII$_1$ to ACII$_5$. All energies are reported in eV relative to the initial state (IS$_c$).
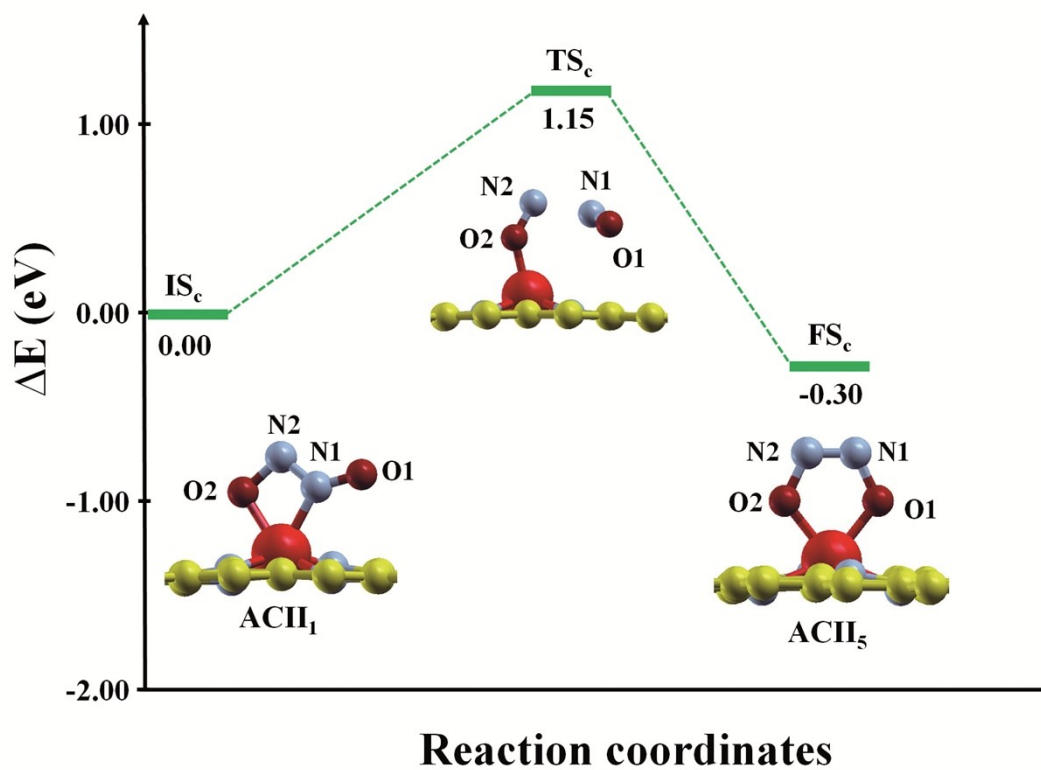
Fig. S18 Energy profile for the recovery of G-Fe-N4 surface by (a) two NO and (b) N_2O. All energies are reported in eV relative to the initial state (IS_d) and distances are in Å. (IS, MS, TS and FS stand for initial, intermediate, transition and final state, respectively.)
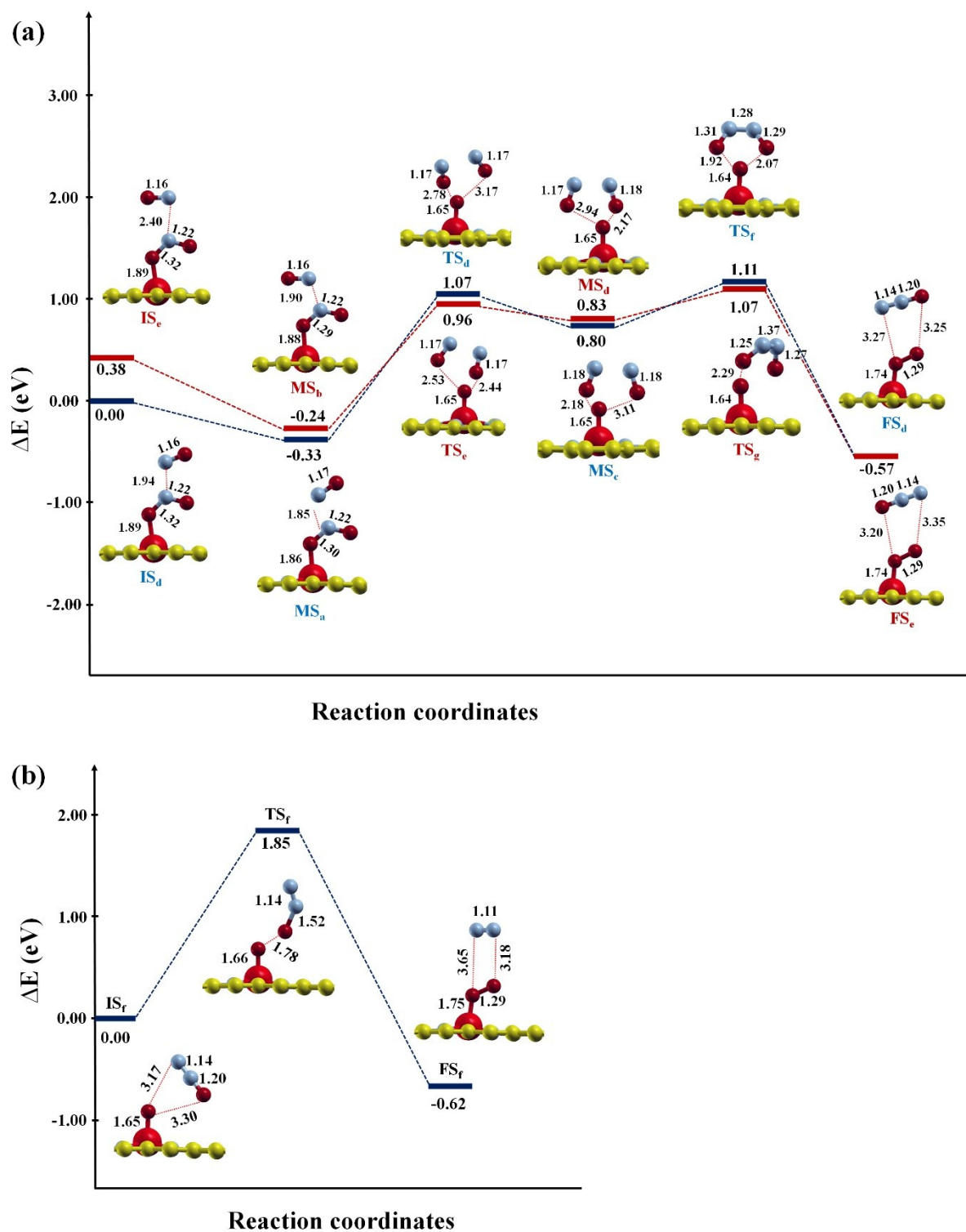
Fig. S19 Energy profile for conversion of acyclic cis-ONNO ($^3A_1$) to $^1N_2O + {}^3O$ in the gas phase from calculations at the TPSS/def2-tzvp level of theory. All energies are reported in eV relative to the initial state (IS_g) and distances are in Å.
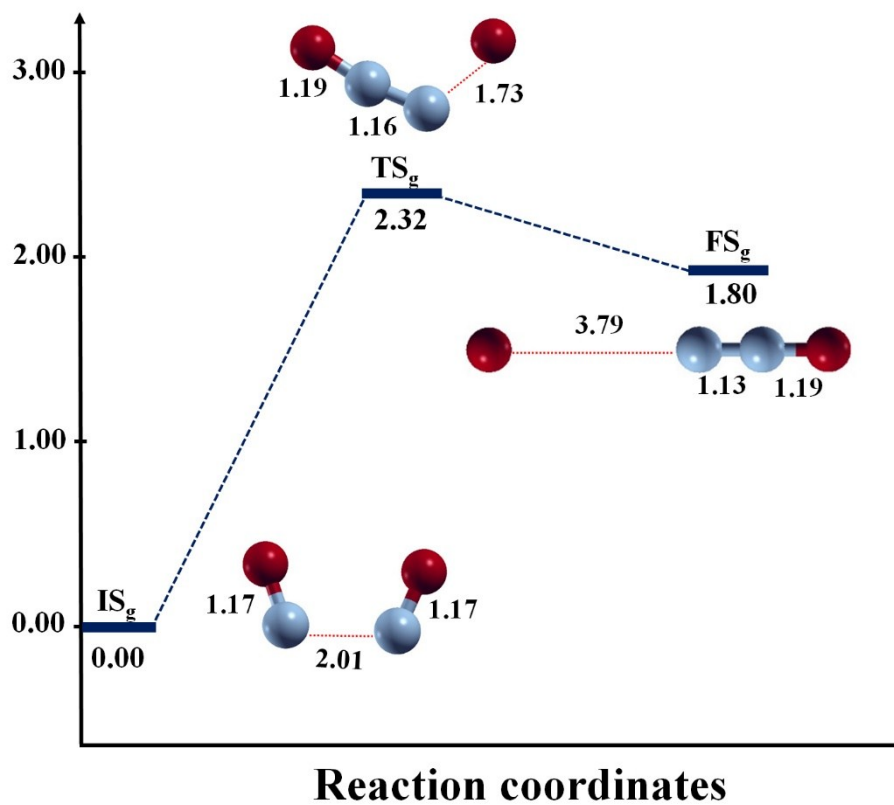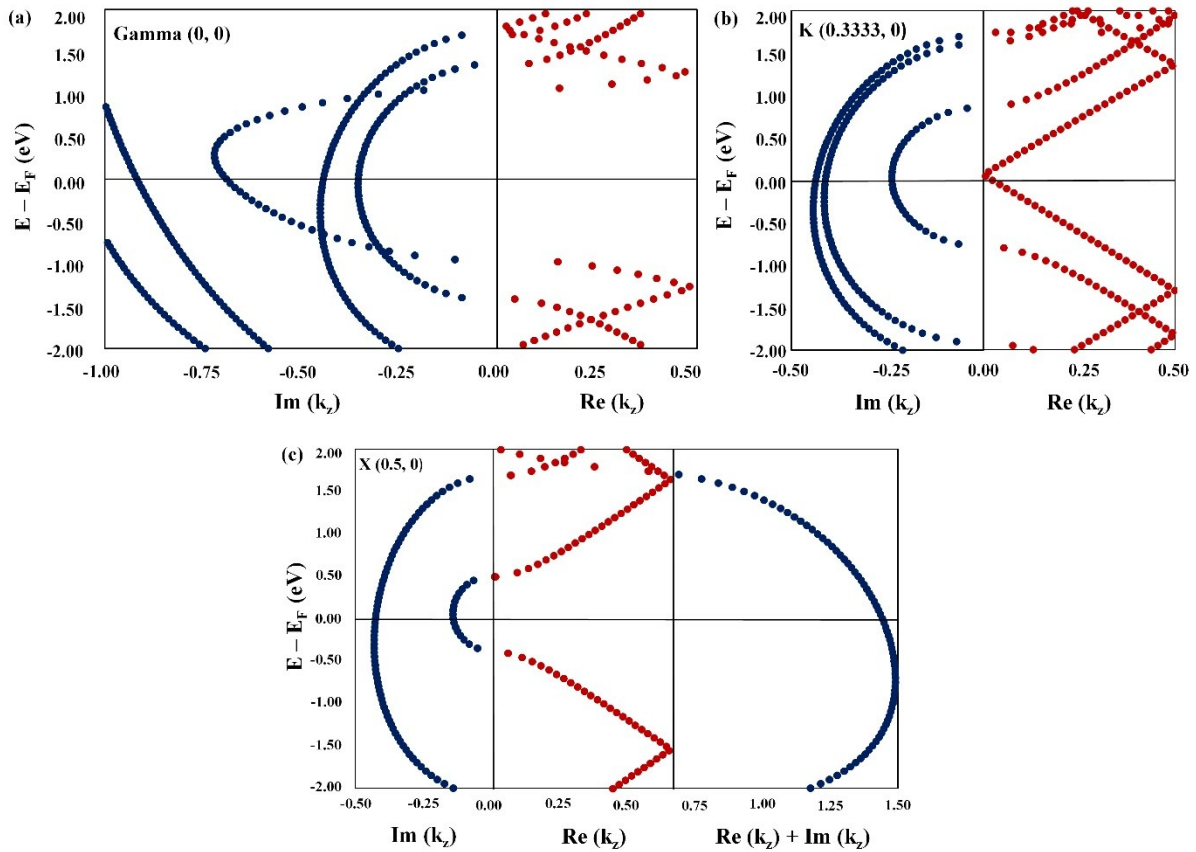
Fig. S20 The complex electronic band structure of pristine graphene (G), for (a) $k_x, k_y(0.0, 0.0)$, (b) $k_x, k_y(0.3333, 0.0)$, and (c) $k_x, k_y(0.5, 0.0)$. This has been obtained using the following parameters: epsproj=0.15 × 10−5, ewind=5.0, and nz1=5 for different k_x, k_y (0, 0), (0.3333, 0) and (0.5, 0)

References

[1] S. Kattel, P. Atanassov, B. Kiefer, *J. Phys. Chem. C*, 2012, **116**, 8161-8166.

[2] W. Orellana, *J. Phys. Chem. C*, 2013, **117**, 9812-9818.

[3] H. A. Duarte, E. Proynov, D. R. Salahub, *J. chem. Phys.*, 1998, **109**, 26-35.

[4] A. R. W. McKellar, J. K. G. Watson, B. J. Howard, *Mol. Phys.*, 1995, **86**, 273-286.

[5] S. G. Kukolich, *J. Mol. Spectrosc.* 1983, **98**, 80-86.

[6] A. F. Cotton, G. Wilkinson, M. Bochmann, C. A. Murillo, *Advanced inorganic chemistry*, Wiley, 6th edn, 1999.

[7] K. P. Huber, G. Herzberg, *Constants of diatomic molecules, Molecular Spectra and Molecular Structure*, Springer, 1979, pp. 8-689.